ELSEVIER

Polymer Vol. 37 No. 13, pp. 2871–2875, 1996
Copyright © 1996 Elsevier Science Ltd
Printed in Great Britain. All rights reserved
0032-3861/96/$15.00 + 0.00

polymer communications

Polyelectrolyte behaviour of dilute xanthan solutions: salt effects on extensional rheology

Steve Carrington and Jeff Odell*
Department of Physics, University of Bristol, Tyndall Avenue, Bristol BS8 1TL, UK

and Len Fisher
School of Interdisciplinary Sciences, University of the West of England, Coldharbour Lane, Bristol BS16 1QY, UK/Department of Physics, University of Bristol, Tyndall Avenue, Bristol BS8 1TL, UK

and John Mitchell and Lee Hartley
Department of Applied Biochemistry and Food Science, University of Nottingham, Sutton Bonington Campus, Loughborough, Leicestershire LE12 5RD, UK
(Received 25 September 1995)

The flow behaviour of xanthan, a biological polyelectrolyte, has widely been reported to be complex, and unlike that of synthetic polyelectrolytes. Most studies have been confined to xanthan concentrations above 0.02% w/w. Using a highly sensitive opposed-jets technique, we have now measured salt concentration effects on the extensional flow behaviour of xanthan in aqueous solution at a concentration of 0.01% w/w. At this low concentration xanthan behaves precisely as expected for a 'normal' polyelectrolyte, collapsing from an extended worm-like conformation to a more compact coil. We suggest that the behaviour at higher xanthan concentrations arises from a disorder–order transition due to intermolecular effects. Copyright © 1996 Elsevier Science Ltd.

(Keywords: xanthan; extensional flow; viscosity)

Introduction

Native xanthan is a high-molecular-weight, anionic, extracellular polysaccharide that is produced by the bacterium *Xanthomonas campestris*[1]. The primary structure is based on a β-1,4-linked glucan backbone[2,3] (cellulosic backbone), with a charged trisaccharide side chain substituted at every second glucose residue. The variation of fermentation and processing conditions lead to different degrees of acetyl substitution (of the mannose residues adjacent to the backbone) and pyruvic acetal substitution (of the terminal mannose units)[4]. The variation in the degree of these substituents has been shown to alter the rheological properties.[5–7].

Xanthan exhibits unusual solution properties, which are significant for industrial purposes. Solutions have a high viscosity and have been reported to exhibit shear and extension thinning[8] as the deformation rate increases (recovering rapidly on the removal of the shearing force). At xanthan concentrations of commercial importance the solution viscosity is high and relatively independent of salt concentration over a large range. This behaviour is atypical of normal polyelectrolytes, which have a highly expanded conformation at low ionic strength and collapse to a more compact coil as the salt concentration is increased (due to charge screening). This change in the hydrodynamic dimensions of the molecule would cause a significant drop in the solution viscosity.

The nature of the secondary structure (or conformation) of xanthan is still a matter of debate in the published literature. The temperature dependence of xanthan solution viscosity is complex. At moderate ionic strengths there is little reduction in viscosity with temperature, whereas most polymer solutions would be expected to show a marked decrease. It has been reported that at low ionic strengths (e.g. in distilled water), the viscosity increases on heating over a specific (and fairly narrow) temperature range[1] and then decreases, indicating that xanthan undergoes a conformational change over this range. This conformational transition has been observed with a variety of techniques[9–15], and has been attributed to an order–disorder transition (in common with other polysaccharide systems[16–20]). The ordered form is helical in nature, but the information available from experiment[11,13,14,21–36] has been unable to prove conclusively whether the structure is a single or double helix, or an aggregate (e.g. a dimer of single helices). As polymer concentration and ionic strength increases, intermolecular ordering (or self-aggregation) through hydrogen bonding and entanglement effects are thought to take on greater importance.

For a perfect single helix, the mass per unit length is ≈ 1000 Daltons nm^{-1}, and the same parameter for the double helix is ≈ 2000 Daltons nm^{-1}. Although measurements indicating both values can be found in the literature, the latter tends to predominate[29,37,38]. The implication may be that an average strandedness of two is present in the ordered state of xanthan.

Ordering by an intermolecular process would be expected to show a concentration dependence. Two critical concentrations have been reported in the literature by different authors. The first transition from

* To whom correspondence should be addressed

dilute to semi-dilute behaviour has been found to occur at a xanthan concentration of between 0.0126 and 0.028% (refs 39–42). The second transition occurs in the range 0.078–0.2% (refs 39–44). The latter transition has been interpreted by some as a critical concentration for co-operative interactions or aggregation[39,41–43]. Xanthan has previously been reported to exhibit behavioural trends typical of normal polyelectrolytes, if the polymer or salt concentration is low enough[1,35,44,45]. However, aggregates have been reported[46,47] at polymer concentrations as low as 0.005%.

To help to clarify this situation, we have now applied the opposed-jets technique to the study of the conformation and extensional rheology of dilute aqueous xanthan solutions, as a function of salt concentration. This technique can be used at lower concentrations than techniques such as differential scanning calorimetry or optical rotation, which have been the basis of many previous conformational studies.

In a preliminary study using extensional flow-fields, a 0.02% w/w xanthan/water solution showed a non-critical, progressive increase in optical retardation with increasing strain rate[48]. Another early study examined the extensional viscosity of xanthan in glycerol/water mixtures[49].

We have previously detailed the use of the opposed-jets technique for the development of idealized extensional flow-fields[50–54]. This technique can enable observation of the orientation, stretching and fracture of high-molecular-weight synthetic polymers and biopolymers. Controlled strain rates in well-characterized uniaxial extensional flow-fields are achieved by sucking solution simultaneously into two jets which face each other with a small separation. At the centre of the flow is a stagnation point where the velocity is zero; the accumulated strain for stream-lines which pass through this point is infinite (see inset, *Figure 3*). The molecular orientation can be assessed by optical retardation. Such experiments reveal that highly flexible chains undergo a critical coil–stretch transition beyond a critical value of strain rate[50]. More rigid molecules, however, show a more gradual orientation increase with strain rate.

The degree of localization of birefringence around the stagnation point is also extremely sensitive to molecular flexibility. The stretching of flexible polymers requires high strains and the birefringence is very sharply localized to those stream-lines which accumulate sufficient strain (close to the stagnation point). Stiffer molecules require less strain to stretch, so they produce a much broader birefringent region. Recently we have reported the development of techniques which enable the simultaneous assessment of macroscopic flow resistance, enabling the complex non-Newtonian effects that occur in extensional flows to be correlated with molecular conformation[51].

The present study is the first detailed application of this techniques a polyelectrolyte biopolymer in dilute aqueous solution. Salt concentration has been selected as a parameter with which to correlate effective extensional viscosity and polymer stretching in stagnation-point extensional flow.

Experimental

Solution preparation. The xanthan sample used in this study was a 'clarified' food grade, Keltrol TF (Kelco, lot number KTLTF 20070V). The powder was dispersed in deionized water (pH 5.1–5.4) using a magnetic stirrer and a high stirring rate. The stirring rate was then reduced, to avoid mechanical degradation, and the polymer was left to dissolve for 24 h at approximately 0°C. The solution was made up to a polymer concentration of 0.01% w/w, and then dialysed against deionized water for 24 h at approximately 0°C. Reagent grade sodium chloride was added to obtain the appropriate salt solution. A fresh solution was used for each experimental run.

Shear viscometry. Measurements of shear viscosity were made using a Bohlin CS rheometer at 25.0 ± 0.1°C, equipped with a double gap geometry. Viscosities at zero shear rate were obtained by extrapolation using the Cross equation.

Opposed jets. The experimental set-up used has been described in detail elsewhere[51]. The apparatus can be used to control strain rates, monitor pressure differences and quantify birefringence around the stagnation point between the jets.

Polymer solution is forced into the flow cell from a reservoir (pressurized by N_2 gas). The solution exits the cell, via the jets, and flows into a piston pump, which acts as a receiving vessel. The flow rate is controlled by the linear rate of travel of the piston. The nominal strain rate ($\dot{\epsilon}$) in the opposed jets can be determined from the flow rate (Q) by:

$$\dot{\epsilon} = \frac{Q}{Ad} \tag{1}$$

where A is the area of the jet entrance and d is the separation between the jets. The opposed jets used had an internal diameter of $D = 0.6$ mm, and a jet separation of $d = 0.4$ mm. The experiments were performed at room temperature (23°C).

The pressure difference across the jets was measured as a function of strain rate.

The optical system used to assess flow-induced birefringence consisted of a 1 mW stabilized He–Ne laser, with the beam focused by a cylindrical lens to create a linear, illuminated region between the jets, centred at the stagnation point. The flow cell was made from stainless steel, with high silicon glass windows located across the beam path. A quarter-wave ($\lambda/4$) plate was placed between the polarizer and the analyser to compensate for any residual birefringence (as a Sénarmont compensator[55]).

The intensity of the birefringent signal, I_s, is given by[56]:

$$I_s = I_0 \sin^2 2\theta \sin^2(\delta/2) \tag{2}$$

where I_0 is the intensity of the incident beam, θ is the angle between the incident polarization direction and the principal axis of the molecular refractive index (chosen to be 45° for maximum signal intensity), which in the opposed-jets flow-field is parallel to the symmetry axis. δ is the average retardation angle, which is related to the birefringence, Δn, by:

$$\Delta n = \frac{\lambda\delta}{2\pi z} \tag{3}$$

where z is the path length through the birefringent line and λ is the wavelength of the incident light (632.8 nm for

He–Ne red laser illumination). Equation (2) shows that the signal intensity varies with the square of δ, providing a quadratic detection method. In this work a linear detection method is used, which involves observing the birefringent signal with a $\lambda/4$ plate between slightly uncrossed polars[57].

In earlier works from this laboratory, quantitative intensity analysis has been limited to an average, global signal from the region between the jets as recorded by a photodiode[50]. The approach used here, giving a more rigorous quantification of intensity, is to utilize a detector with many independent segments, measuring the intensity of light incident upon them. By focusing an image of the birefringent line onto the plane of such a detector, profiles of the line may be digitally recorded.

The detector used was a charge-coupled device (CCD) consisting of a linear array of 256 light-sensitive pixels, each measuring 13 μm × 13 μm, arranged perpendicular to the axis of the cylindrical birefringent region. After calibration and consideration of background contribution to the measured intensities, retardation profiles at different strain rates were obtained[52].

Results and discussion

Plots of zero-shear viscosity against concentration (not shown) gave values for the first transition of 0.025–0.03% w/w in water and 0.04–0.06% w/w in 0.1 M NaCl, confirming that our extensional flow measurements at 0.01% w/w were clearly in the dilute regime.

Figure 1a shows the flow-induced retardation as a function of strain rate and radial distance from the stagnation point for xanthan solution in dialysed deionized water. This shows an optical retardation which is delocalized around the stagnation point. This evidence of birefringence at large radial distances from the stagnation point is consistent with a low strain to stretch and with a worm-like expanded polyelectrolytic behaviour. The broad wings of retardation at the greatest radii are of opposite sign of birefringence to that at the stagnation point and are likely to be due to the orientation of individual molecules on the incoming axis, which also indicates that little strain is required to stretch the molecules.

Figure 1b corresponds to the same system, but in 10^{-2} M NaCl. In contrast to the behaviour of the solution in water, the strain rate required to stretch the xanthan molecules is increased and the negative retardation of the wings is reduced to near zero. This behaviour is consistent with a classical collapse of the expanded polyelectrolyte under the increasing screening effect of counter-ions[54,58,59]. The birefringent region is still very broad compared with that found for highly flexible molecules such as atactic polystyrene[52], indicating that even the collapsed xanthan molecule is still relatively stiff.

Figure 2a shows the peak retardation at the stagnation point, together with the peak width at half-height, as a function of strain rate for a 0.01% xanthan solution in deionized water. The change in retardation with increasing strain rate demonstrates an increasing orientation of the molecules in the flow-field, until saturation is reached in the limit of high molecular orientation. The width of the line can be used to estimate the molecular strain required to stretch the molecule, and therefore the molecular flexibility. In the present case the width of

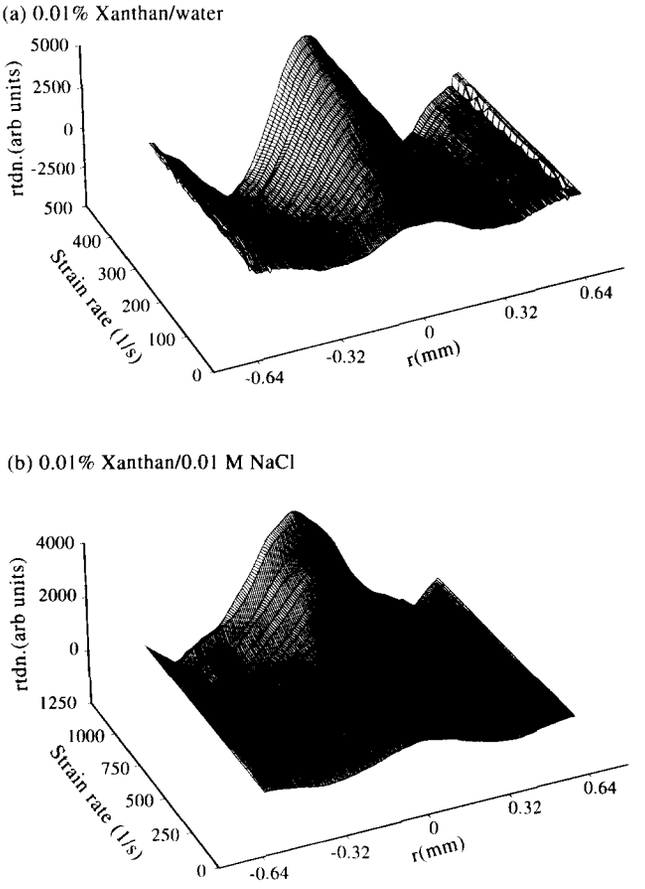

Figure 1 Flow-induced retardation as a function of strain rate and radial distance r from the stagnation point. 0.01% xanthan in: (a) dialysed, deionized water and (b) 0.01 M NaCl. Arbitrary retardation units are the same in both figures

the line around the stagnation point is partially obscured by the overlaying 'wings' from the incoming axis. A proper estimate of line width and flexibility will require a deconvolution of these two effects. The half-height line width is, however, of the order of 250 μm; this should be contrasted with a line width of approximately 10 μm for highly flexible atactic polystyrene, and virtually complete delocalization for rigid rod poly(*p*-phenylene-benzbis-thiazole)[50]. The localization of the birefringence of xanthan is thus consistent with expectations for the stretching and orientation of expanded worm or rod-like molecules. The half-height birefringent stream-line is known from a detailed finite element fluid flow analysis[60] of the jets to correspond to a fluid strain of ≈ 10. It is likely that the molecular strain to stretch in the free-draining xanthan molecule is comparable. *Figure 2b* corresponds to the same system, but in 10^{-2} M NaCl, and clearly shows the later onset of stretching in the salt solution, corresponding to the reduced relaxation time of the collapsed worm-like molecule. As discussed above, this is consistent with a classical collapse of the expanded polyelectrolyte due to screening.

Figure 3 shows the pressure difference across the jets as a function of strain rate for water, xanthan in deionized water and xanthan in 10^{-2} M NaCl. The increasing extensional viscosity with strain rate (dilatancy) is at variance with previous results on xanthan in semi-dilute solutions (0.056%)[8], but is just the behaviour expected for a semi-flexible molecule. Again, the rheological effects

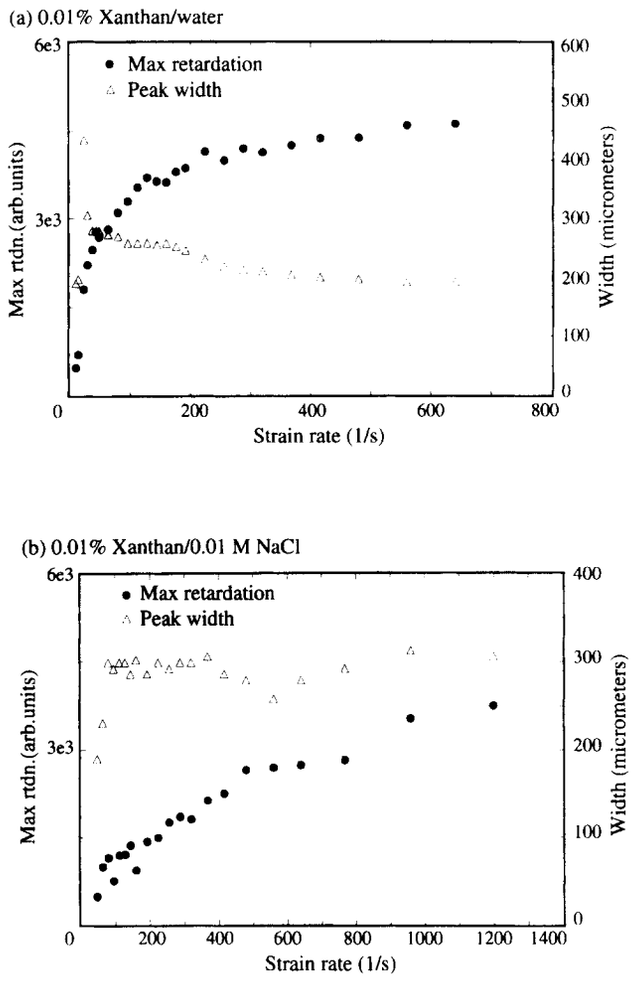

Figure 2 The maximum retardation at the stagnation point (●) and the peak width at half-height (Δ) as a function of strain rate. 0.01% xanthan in: (a) dialysed, deionized water and (b) 0.01 M NaCl

are delayed in salt solution, as has been observed for other polyelectrolyte systems such as hydrolysed poly(acrylamide)[54] and poly(styrene sulfonate)[58], indicating a classical polyelectrolyte behaviour at these high dilutions.

The effects of the collapse of the xanthan molecule with added salt seen in the jets are also reflected in the

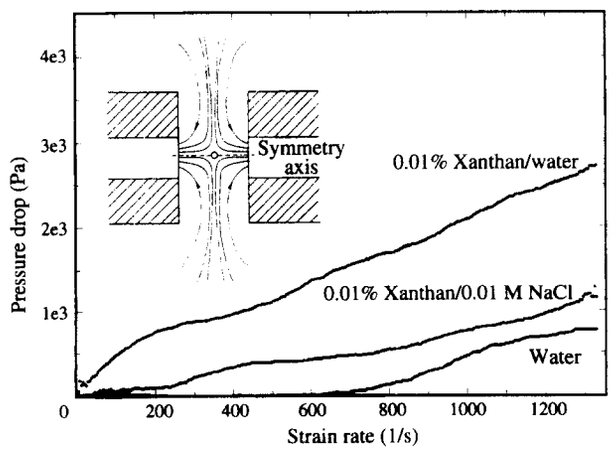

Figure 3 The pressure difference across the jets, as a function of strain rate for water, 0.01% xanthan solution in dialysed, deionized water, and in 0.01 M NaCl. The inset shows a schematic representation of the geometry and the stream-lines of the opposed jets

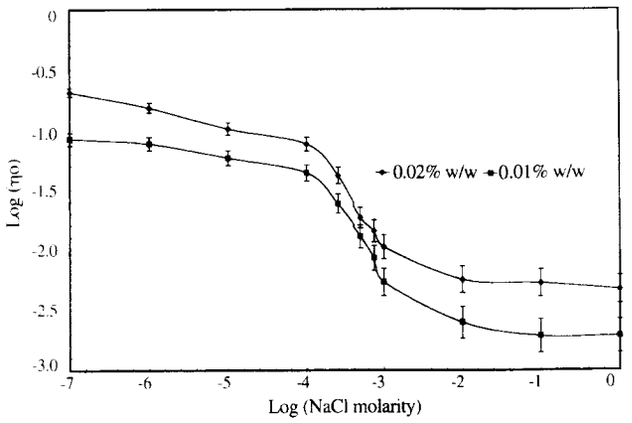

Figure 4 Zero-shear viscosity of xanthan solutions plotted against NaCl concentration. Results are the mean of two or three runs. Measurements were made at 25.0 ± 0.1°C

shear viscosity. *Figure 4* shows the zero-shear viscosity measured at 0.01% and 0.02% w/w as a function of the concentration of added NaCl. The plot shows a dramatic collapse in the zero-shear viscosity over the same range of added salt concentration.

Conclusions

At sufficiently high dilutions (0.01% w/w) xanthan behaves as a normal polyelectrolyte, showing a progressive collapse with increasing ionic strength, which is reflected in reduced shear and extensional viscosities. This suggests that the behaviour observed at higher concentrations and attributed to the presence of an ordered state is inter- rather than intramolecular in character.

Acknowledgement

We gratefully acknowledge the support of the BBSRC for this work.

References

1 Jeanes, A., Pittsley, J. E. and Senti, F. R. *J. Appl. Polym. Sci.* 1961, **5**, 519
2 Jansson, P. E., Kenne, L. and Lindberg, B. *Carbohydr. Res.* 1975, **45**, 275
3 Melton, L. D., Mindt, L., Rees, D. A. and Sanderson, G. R. *Carbohydr. Res.* 1976, **46**, 245
4 Sandford, P. A., Pittsley, J. E., Knutson, C. A., Watson, P. R., Cadmus, M. C. and Jeanes, A. in 'Extracellular Microbial Polysaccharides' (Eds P. A. Sandford, and A. Laskin), ACS Symposium Series 45, American Chemical Society, Washington DC, 1977, p. 192
5 Holzwarth, G. and Ogletree, J. *Carbohydr. Res.* 1979, **76**, 277
6 Smith, I. H., Symes, K. C., Lawson, C. J. and Morris, E. R. *Int. J. Biol. Macromol.* 1981, **3**, 129
7 Kulicke, W.-M., Oertel, R., Otto, M., Kleinitz, W. and Littmann, W. *Erdoel Kohle, Erdgas Petrochem.* 1990, **43**, 471
8 Clark, R. C. in 'Gums and Stabilizers in the Food Industry' (Eds G. O. Phillips, D. J. Wedlock and P. A. Williams), IRL Press, Oxford, 1991, Vol. 6
9 Morris, E. R., Rees, D. A., Young, G., Walkinshaw, M. D. and Darke, A. *J. Mol. Biol.* 1977, **110**, 1
10 Holzwarth, G. *Biochem.* 1976, **15**, 4333
11 Milas, M. and Rinaudo, M. *Carbohydr. Res.* 1979, **76**, 189
12 Southwick, J. G., McDonnell, M. E., Jamieson, A. M. and Blackwell, J. *Macromolecules* 1979, **12**, 305
13 Norton, I. T., Goodall, D. M., Morris, E. R. and Rees, D. A. *J. Chem. Soc., Chem. Commun.* 1980, 545
14 Norton, I. T., Goodall, D. M., Frangou, S., Morris, E. R. and Rees, D. A. *J. Mol. Biol.* 1984, **175**, 371
15 Bezemer, L., Ubbink, J. B., de Kooker, J. A., Kuil, M. E. and Leyte, J. C. *Macromolecules* 1993, **26**, 6436

16 Rees, D. A. and Scott, W. E. *J. Chem. Soc. B* 1971, 469
17 Rees, D. A., Scott, W. E. and Williamson, F. B. *Nature* 1970, **227**, 390
18 Rees, D. A., Steel, I. W. and Williamson, F. B. *J. Polym. Sci. C* 1969, **28**, 261
19 Bryce, T. A., McKinnon, A. A., Morris, E. R., Rees, D. A. and Thom, D. *Faraday Discuss. Chem. Soc.* 1974, **57**, 221
20 Dea, I. C. M., McKinnon, A. A. and Rees, D. A. *J. Mol. Biol.* 1972, **68**, 153
21 Moorhouse, R., Wilkinshaw, M. D. and Arnott, S. in 'Extracellular Microbial Polysaccharides' (Eds P. A. Sandford and A. Laskin), ACS Symposium Series 45, American Chemical Society, Washington DC, 1977, p. 90
22 Okuyama, K., Arnott, S., Moorhouse, R., Wilkinshaw, M. D., Atkins, E. D. T. and Wolf-Ullish, Ch. in 'Fiber Diffraction Methods' (Ed. Ch. Wolf-Ullish), ACS Symposium Series 141, American Chemical Society, Washington DC, 1980, p. 411
23 Holzwarth, G. and Prestridge, F. G. *Science Washington DC* 1977, **197**, 757
24 Stokke, B. T., Elgsaeter, A. and Smidsrød, O. *Int. J. Biol. Macromol.* 1986, **8**, 217
25 Stokke, B. T., Smidsrød, O. and Elgsaeter, A. *Biopolymers* 1989, **28**, 617
26 Milas, M. and Rinaudo, M. *Polym. Bull.* 1984, **12**, 507
27 Milas, M. and Rinaudo, M. *Carbohydr. Res.* 1986, **158**, 191
28 Paoletti, S., Cesàro, A. and Delben, F. *Carbohydr. Res.* 1983, **123**, 173
29 Sato, T., Norisuye, T. and Fujita, H. *Polym. J.* 1984, **16**, 341
30 Sato, T., Kojima, S., Norisuye, T. and Fujita, H. *Polym. J.* 1984, **16**, 423
31 Sato, T., Norisuye, T. and Fujita, H. *Polym. J.* 1985, **17**, 729
32 Liu, W. and Norisuye, T. *Int. J. Biol. Macromol.* 1988, **10**, 44
33 Liu, W. and Norisuye, T. *Biopolymers* 1988, **27**, 1641
34 Lecourtier, J., Chauveteau, G. and Muller, G. *Int. J. Biol. Macromol.* 1986, **8**, 306
35 Muller, G., Anrhourrache, M., Lecourtier, J. and Chauveteau, G. *Int. J. Biol. Macromol.* 1986, **8**, 167
36 Besio, G. J., Leavesley, I. M. and Prud'homme, R. K. *J. Appl. Polym. Sci.* 1987, **33**, 825
37 Holzwarth, G. *Carbohydr. Res.* 1978, **66**, 173
38 Paradossi, G. and Brant, D. A. *Macromolecules* 1982, **15**, 874
39 Cuvelier, G. and Launay, B. *Adv. Rheol., IX Int. Congr. Rheol.* 1984, **2**, 247
40 Milas, M., Rinaudo, M., Knipper, M. and Schuppiser, J. L. *Macromolecules* 1990, **23**, 2506
41 Jamieson, A. M., Southwick, J. G. and Blackwell, J. *J. Polym. Sci., Polym. Phys. Edn* 1982, **20**, 1513
42 Southwick, J. G., Jamieson, A. M. and Blackwell, J. *Macromolecules* 1981, **14**, 1728
43 Rochefort, W. E. and Middleman, S. *J. Rheol.* 1987, **31**, 337
44 Whitcomb, P.J. and Macosko, C. W. *J. Rheol.* 1978, **22**, 493
45 Southwick, J. G., Jamieson, A. M. and Blackwell, J. *Carbohydr. Res.* 1982, **99**, 117
46 Meyer, E. L., Fuller, G. G., Clark, R. C. and Kulicke, W.-M. *Macromolecules* 1993, **36**, 504
47 Southwick, J. G., Lee, H., Jamieson, A. M. and Blackwell, J. *Carbohydr. Res.* 1980, **84**, 287
48 Ross-Murphy, S. B., Morris, V. J. and Morris, E. R. *Faraday Symp. Chem. Soc.* 1983, **18**, 115
49 Fuller, G. G., Cathey, C. A., Hubbard, B. and Zebrowski, B. E. *J. Rheol.* 1987, **31**, 235
50 Keller, A. and Odell, J. A. *Colloid Polym. Sci.* 1985, **263**, 181
51 Odell, J. A., Müller, A. J., Narh, K. A. and Keller, A. *Macromolecules* 1990, **23**, 3092
52 Tatham, J. P. 'Extensional flow dynamics of macromolecules of different flexibilities in solution', *Ph.D. Dissertation*, University of Bristol, 1993
53 Odell, J. A., Müller, A. J. and Keller, A. in 'Polymers in Aqueous Media' (Ed. J. E. Glass), Advances in Chemistry 1989, **223**, 193
54 Odell, J. A., Müller, A. J. and Keller, A. *Polymer* 1988, **29**, 1179
55 Hartshorne, N. H. and Stuart, A. 'Crystals and the Polarising Microscope', Edward Arnold, London, 1960
56 Fredericq, E. and Houssier, C. 'Electric Dichroism and Electric Birefringence', Clarenden Press, Oxford, 1973
57 Riddiford, C. L. and Jerrard, H. G. *J. Phys. D.: Appl. Phys.* 1970, **3**, 1314
58 Miles, M. J., Tanaka, K. and Keller, A. *Polymer* 1983, **24**, 1081
59 Dunlap, P. N., Wang, C.-H. and Leal, L. G. *J. Polym. Sci., Part B: Polym. Phys.* 1987, **25**, 2211
60 Carrington, S. P. 'The extensional flow properties of polymer solutions', *Ph.D. Thesis*, University of Bristol, 1995